

# Phase transformations in composite films of the system Se-Cu, obtained using explosive crystallization and thermal annealing

© V.Ya. Kogai, T.N. Mogileva, A.E. Fateev, G.M. Mikheev

Udmurt Federal Research Center, Ural Branch of the Russian Academy of Sciences,  
426067 Izhevsk, Russia

E-mail: vkogai@udman.ru

Received January 19, 2022

Revised February 14, 2022

Accepted February 14, 2022

The results of experimental studies of the phase transformation in composite films of the Se-Cu system obtained in vacuum as a result of the sequential thermal deposition of selenium and copper on a glass substrate are presented. At a fixed thickness of the selenium layer (45 nm), the effect of the thickness of the copper layer (40–115 nm) on the phase composition of the synthesized films formed as a result of explosive crystallization occurring during the interaction of hot copper clusters with low-melting selenium was studied. It was found that the subsequent thermal annealing of the synthesized films is accompanied by a significant change in their phase composition and optical transmission spectra.

**Keywords:** phase transformations, composite films of the Se-Cu system, explosive crystallization, thermal annealing, optical properties.

DOI: 10.21883/SC.2022.06.53533.9802

## 1. Introduction

Copper selenides attract increasingly greater attention thanks to their composition and structural universality. The most well-studied are stoichiometric ( $\text{CuSe}_2$ ,  $\text{CuSe}$ ,  $\text{Cu}_3\text{Se}_2$  and  $\text{Cu}_2\text{Se}$ ) and non-stoichiometric ( $\text{Cu}_{2-x}\text{Se}$ ) compounds, where  $0 < x < 2$  [1]. Copper selenide has unique photoelectric and optical properties and is widely used in various electronic and optoelectronic devices [2,3]. Depending on production methods, thin copper selenide films are crystallized in rhombic [4], cubic, hexagonal [5] and tetragonal [6] structures. Copper selenide is obtained by mechanochemical synthesis and compaction by means of spark plasma sintering and hot pressing [7], selenization [8], electrodeposition [9], solvothermal method [10], pulsed laser deposition [11], sol-gel method [12], chemical deposition from aqueous solutions [13]. Most of the above-mentioned methods for copper selenide synthesis require complex processing equipment with creation of deep vacuum and high temperatures.

One of the promising methods for obtaining thin crystalline copper selenide films is film synthesis in the explosive crystallization mode during formation of a Se/Cu film structure in vacuum. This method makes it possible to obtain copper selenide at room temperature (substrate temperature 25°C) [14].

We have demonstrated earlier [15] that the phase composition of synthesized films can be controlled by changing the ratio of copper and selenium atoms in a sample taking into account their atomic radii. It was also established that irradiation of thin stoichiometric CuSe and composite CuSe/Se films with femtosecond laser pulses can excite photoinduced current pulses in them, which depend on polarization of incident radiation [16–19]. It is very

interesting to study the circular photoinduced current, which depends on rotation direction of the electric field vector of incident radiation observed in the mentioned thin-film structures [17,18,20]. By varying the phase composition of synthesized films, efficiency of circular photoinduced current generation can be controlled and mechanisms of its occurrence can be studied.

Composite films of copper selenide with a different phase composition can be obtained not only by changing the ratio of selenium and copper layer thicknesses, but also by their subsequent thermal annealing. The possibility of efficient use of composite films of the Se-Cu system depends on their optical properties, particularly on optical band gap  $E_g$ . According to the literature data [21–24],  $E_g$  in copper selenide films may vary in a wide range from 2 to 3 eV and from 1.1 to 1.5 eV under direct and indirect optical transitions respectively.

It was also reported in [25] that CuSe nanoparticles have  $E_g \sim 4$  eV in regions of direct optical transitions and 1.87 eV in regions of indirect transitions. The authors of [22] believe that large values of  $E_g$  in regions of indirect optical transitions are associated with the quantum confinement effect, due to which electrons are localized in individual crystallites.

The goal of the present paper is to study the phase transformations in composite films of the Se-Cu system during explosive crystallization and subsequent thermal annealing, as well as to study their optical properties.

## 2. Experimental procedure

A Se/Cu film structure was formed by vacuum-thermal evaporation. Vacuum in the working chamber and glass

substrate temperature were  $10^{-3}$  Pa and  $25^{\circ}\text{C}$  respectively. The Se and Cu films were deposited in a single vacuum cycle by successive evaporation of Se weighed portions, and then Cu weighed portions onto glass substrates sized  $20 \times 15 \times 1.5$  mm.

Our paper [15] describes the making of composite CuSe/*a*-Se films (*a*-Se—amorphous selenium) by the vacuum-thermal evaporation method. Evaporation of the Se weighed portion was performed using a box-type tantalum effusion evaporator. The Se deposition rate was 9.5 nm/s. We used a tubular effusion evaporator to evaporate the Se weighed portion. Thereat, the Se film deposition rate was 20 nm/s. By changing the weight of the Se and Cu weighed portions and, consequently, their thickness ratio ( $d_{\text{Se}}/d_{\text{Cu}}$ ), nanocrystalline copper selenide films having a different phase composition can be obtained.

Thermal annealing of films, obtained by explosive crystallization, was performed in the working chamber under  $10^{-3}$  Pa vacuum. The authors of [26] found that a complete transformation of monoclinic selenium into trigonal selenium at  $120^{\circ}\text{C}$  occurs within 1 h, while at  $65^{\circ}\text{C}$  this process lasts for over 17 days. Moreover, it was shown in [7] that a transition of the  $\alpha$ -phase of  $\text{Cu}_2\text{Se}$  to  $\beta$ - $\text{Cu}_2\text{Se}$  starts already at  $140^{\circ}\text{C}$ . Based on the aforesaid, we chose the temperature of  $140^{\circ}\text{C}$  and annealing time of 30 min respectively.

Thickness of the Se and Cu films was determined using the ellipsometric method.

The films' crystal structure and phase composition was studied at room temperature using a D2 PHASER diffractometer manufactured by Bruker.  $\text{CuK}\alpha$ -radiation was used ( $\lambda = 0.154$  nm). The universal DIFFRAC.EVA program was used for smoothing of the diffraction curves and subtraction of the background caused by X-ray scattering on the glass substrate. Then the phase composition of the synthesized films was identified.

Transmission spectra of the copper selenide films obtained on glass were recorded using a SF-56 spectrophotometer. Transmission spectra were taken in relation to a clean glass substrate in the wavelength range of 400–1100 nm with a 1 nm interval. Optical parameters, such as extinction coefficient  $k$ , absorption coefficient  $\alpha$  and optical band gap  $E_g$ , were determined from the transmission spectra of the Se-Cu composite films. The extinction coefficient was calculated using formula  $k = 2.303 \log(1/T)\lambda/4\pi d$ , where  $T$  — transmission coefficient,  $\lambda$  — wavelength,  $d$  — film thickness. The absorption coefficient  $\alpha$  was determined using formula  $\alpha = 4\pi k/\lambda$ . The optical study data was analyzed based on the Bardin ratio [27], where the film absorption coefficient  $\alpha$  is associated with energy of incident photons  $h\nu$  by the equation  $(\alpha h\nu)^m = A(h\nu - E_g)$ , where  $A$  — coefficient dependent on film transmittance and thickness,  $E_g$  — optical band gap,  $m$  — coefficient which characterizes the optical transition type ( $m = 2$  — direct optical transition,  $m = 1/2$  — indirect optical transition). Values of  $E_g$  for synthesized films were determined by plotting the spectral dependence of quantity

$(\alpha h\nu)^m$  on  $h\nu$ , followed by extrapolation of the obtained curve by a linear function up to the abscissa axis (see, for instance, [28]).

### 3. Results and discussion

Composite films of the Se-Cu system were obtained by solid-phase synthesis during formation of a Se/Cu film structure in a single vacuum cycle. Thereat, the selenium film thickness in all samples was identical and equal to 45 nm, while the copper film thickness varied from 40 to 115 nm.

An increase of Se deposition rate to 20 nm/s caused an increase of defect concentration in the Se film and, consequently, an increase of elastic stress energy in it. Relaxation of this energy under deposition of Cu clusters onto a Se films triggered a solid-phase chemical reaction between copper and selenium with the formation of CuSe and crystallization of excess amorphous selenium with the formation of a monoclinic  $\text{Se}_8$  phase. As a result, the composite film obtained at the Se deposition rate of 20 nm/s contains a hexagonal CuSe phase and a monoclinic  $\text{Se}_8$  phase, as well as an amorphous *a*-Se phase (see Fig. 1, curve 1).

It should be noted that we have reported [29] the triggering of a solid-phase chemical reaction in a  $\text{Cu}/\text{As}_2\text{Se}_3$  film structure by elastic stress energy, and the mechanism of action of positive feedback between a chemical reaction in a solid body and elastic stresses. It is also known that a monoclinic  $\text{Se}_8$  phase is found in thin (up to 120 nm) Ge-Se polycrystal films obtained by vacuum-thermal evaporation on a glass substrate being at room temperature. The film deposition rate was 10 nm/s [30].

Since the Cu evaporation temperature  $1260^{\circ}\text{C}$  is significantly higher than the selenium melting temperature  $217^{\circ}\text{C}$ , a liquid interlayer may form on the layer interface during Cu deposition onto the Se layer. The formation of a liquid interlayer leads to an abrupt increase of the rate of the chemical reaction between Cu and Se. This leads to intensive growth of nucleating crystals of copper selenide and a significant release of phase transformation thermal energy. Besides, elastic stress energy in a film system also increases due to different molar volumes of crystalline phases in it. The cooperative effect of phase transformation thermal energy and elastic stress energy causes development of explosive crystallization [31].

Figure 1 shows the X-ray diffraction patterns for the Se(45 nm)/Cu(40 nm) film structure obtained by explosive crystallization (curve 1), and the same film after its annealing at  $140^{\circ}\text{C}$  for 30 min (curve 2). The X-ray diffraction pattern for the initial synthesized film has diffraction peaks which correspond to the lines of reflection from the hexagonal CuSe phase and monoclinic  $\text{Se}_8$  phase (Fig. 1, curve 1). It is seen that the CuSe phase is prevailing. According to the reference data, CuSe pertains to the space group of symmetry

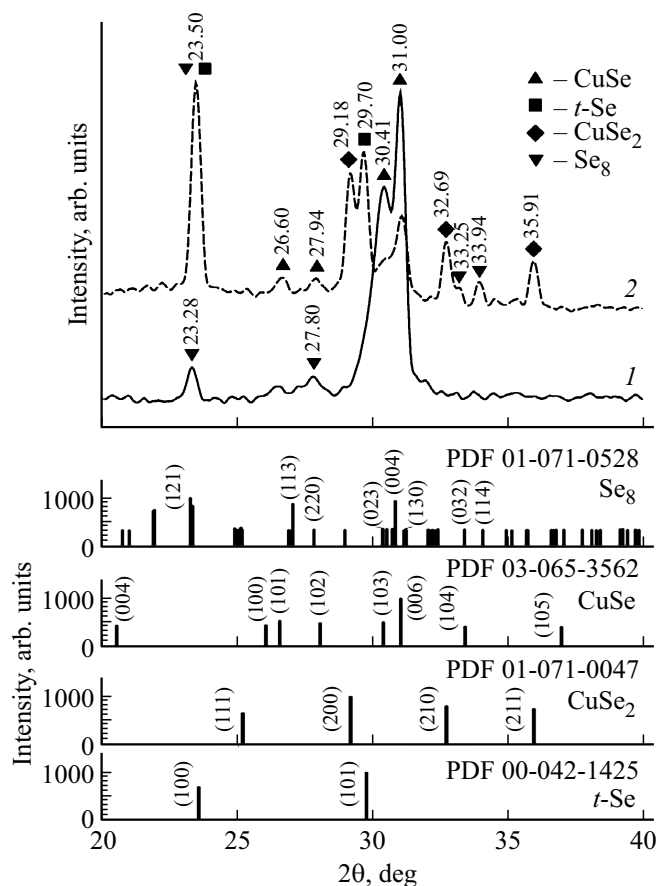


**Figure 1.** Diffraction patterns of the Se(45 nm)/Cu(40 nm) film structure after explosive crystallization (1) and their thermal annealing at 140°C for 30 min (2), as well as reference X-ray diffraction patterns and  $hkl$  of the found phases under excitation by X-ray radiation  $\text{CuK}\alpha$ .

$P63/mmc$  (PDF 03-065-3562) having the crystal lattice parameters  $a = 0.3948$  nm,  $c = 1.728$  nm. Texturized growth of CuSe crystallites in planes (103) and (006), which correspond to the scattering angles  $2\theta = 30.4$  and  $31^\circ$  (Fig. 1, curve 1). The monoclinic  $\text{Se}_8$  phase having the crystal lattice parameters  $a = 0.9054$  nm,  $b = 0.9083$  nm and  $c = 1.1601$  nm pertains to the space group of symmetry  $P21/n$  (PDF 01-071-0528). The diffraction pattern in Fig. 1 (curve 1) shows this phase as a line with the scattering angle  $2\theta = 23.28^\circ$ .  $\text{Se}_8$  crystallites grow in plane (121). The diffraction pattern for the synthesized film shows no reflections from Cu crystallites, which means that copper dissolves in the selenium film with the formation of CuSe crystallites. Thus, the initial synthesized film obtained by explosive crystallization is a composite containing two crystalline CuSe,  $\text{Se}_8$  phases and an amorphous  $a$ -Se phase. Subsequent thermal annealing of the same film at 140°C for 30 min causes diffraction peaks from the trigonal Se phase ( $t$ -Se). This is confirmed by two intensive peaks at the scattering angles  $2\theta = 23.5$  and  $29.7^\circ$ . These peaks occur due to X-ray radiation scattering on the crystal planes (100)

and (101)  $t$ -Se (Fig. 1, curve 2). The  $t$ -Se phase having the crystal lattice parameters  $a = 0.4358$  nm and  $c = 0.4950$  nm pertains to the space group of symmetry  $P3_121$  (PDF 00-042-1425). This phase nucleates and forms during thermal annealing due to crystallization of the amorphous Se phase, which does not manifest itself on the diffraction pattern as separate peaks. It should be noted that texturized growth of  $t$ -Se crystallites occurs in plane (100) (Fig. 1, curve 2). In addition to the above-mentioned peaks, the diffraction pattern for the annealed film shows other peaks, which correspond to the lines of reflection from the cubic  $\text{CuSe}_2$  phase, which pertains to the space group of symmetry  $Pa-3$  (PDF 01-071-0047) having the crystal lattice parameters  $a = 0.6116$  nm (Fig. 1, curve 2). This is confirmed by peaks with the scattering angles  $2\theta = 29.18$ ,  $32.69$  and  $35.91^\circ$ .

Figure 2, *a* shows the optical transmission spectra for the synthesized film structure before (curve 1) and after (curve 2) thermal annealing. It is seen that the film transmission coefficient after thermal annealing decreases considerably at all wavelengths in a wide spectral range from 400 to 1100 nm. This can be explained by a change in the film phase composition after thermal annealing. In particular, it is known that a transformation of amorphous selenium into crystalline  $t$ -Se is accompanied with a considerable increase of the film material absorbance in the visible and near-infrared regions [32].

$E_g$  of the obtained films was determined using the optical transmission spectra shown in Fig. 2, *a*. The obtained values of  $E_g$  for the composite  $\text{CuSe}/\text{Se}_8/a$ -Se film (obtained before annealing) in regions of direct and indirect optical transitions were 2.2 and 1.87 eV respectively. After its heat treatment, a more complex composite  $\text{CuSe}/\text{Se}_8/t$ -Se/ $\text{CuSe}_2$  film formed, whose values of  $E_g$  in regions of direct and indirect optical transitions were 2.18 and 1.45 eV, respectively.

Thus,  $\text{Se}_8$  and CuSe crystallites, as well as amorphous Se form in the Se(45 nm)/Cu(40 nm) film structure during explosive crystallization. Subsequent thermal annealing of the synthesized film structure causes the formation of an optically denser nanocomposite film that simultaneously contains four crystalline phases  $\text{Se}_8$ ,  $t$ -Se, CuSe and  $\text{CuSe}_2$ .

The experiments show that thin composite films having a different phase composition can be obtained by changing the ratio of Se and Cu layer thicknesses ( $d_{\text{Se}}/d_{\text{Cu}}$ ) in the Se/Cu film structure and by their subsequent thermal annealing.

Figure 3 (curve 1) shows the diffraction pattern for the Se(45 nm)/Cu(90 nm) film structure recorded directly after deposition. It does not have peaks corresponding to  $\text{Se}_8$ , but has peaks corresponding to the tetragonal  $\text{Cu}_3\text{Se}_2$  phase with angles  $2\theta = 25.07$ ,  $28.79$ ,  $35.06$ ,  $47.60$  and  $51.42^\circ$ , as well as the hexagonal CuSe phase with angles  $2\theta = 30.21$  and  $30.93^\circ$ . These phases occur as a result of explosive crystallization. A comparison of the reference X-ray diffraction patterns for the revealed phases (see Fig. 3) with the recorded diffraction pattern

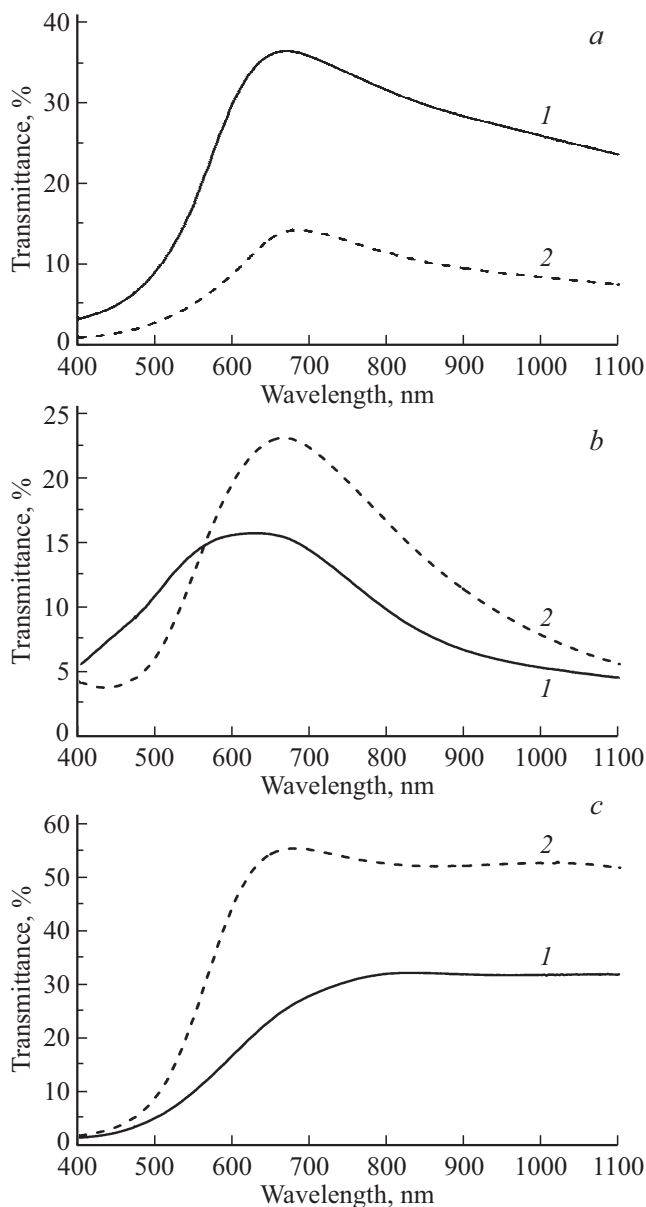


**Figure 2.** Transmission spectra ( $T$ ) for the composite films after explosive crystallization (1) and their thermal annealing at  $140^{\circ}\text{C}$  for 30 min (2): *a* — Se(45 nm)/Cu(40 nm); *b* — Se(45 nm)/Cu(90 nm); *c* — Se(45 nm)/Cu(115 nm).

for the synthesized film makes it possible to conclude that explosive crystallization causes texturized growth of  $\text{Cu}_3\text{Se}_2$  and CuSe crystallites along planes (101) and (006) respectively. The prevailing phase in the synthesized film is  $\text{Cu}_3\text{Se}_2$  having the crystal lattice parameters  $a = 0.6403$  nm and  $c = 0.4277$  nm, which pertains to the space group of symmetry  $P-421m$  (PDF 00-047-1745). The space group of symmetry and crystal lattice parameters for the hexagonal CuSe phase are given above. Subsequent thermal annealing of the obtained  $\text{Cu}_3\text{Se}_2/\text{CuSe}$  film at  $140^{\circ}\text{C}$  for 30 min causes an almost complete transformation of the tetragonal  $\text{Cu}_3\text{Se}_2$  phase into the hexagonal CuSe phase. It is

confirmed by disappearance of the peaks at scattering angles  $2\theta = 25.07, 28.79, 47.60$  and  $51.42^{\circ}$ , which pertain to the  $\text{Cu}_3\text{Se}_2$  phase (see Fig. 3, curve 2). This results in the formation of a polycrystalline film structure which almost fully consists of CuSe crystallites predominantly oriented in plane (006). The transformation of  $\text{Cu}_3\text{Se}_2$  into CuSe under thermal annealing can be explained by a solid-phase reaction during which the Se atoms from its amorphous phase, present in the film structure after vacuum-thermal deposition, interact chemically with  $\text{Cu}_3\text{Se}_2$  molecules to form CuSe.

The optical transmission spectra for the Se(45 nm)/Cu(90 nm) film structure, recorded before and after its thermal annealing, are shown in Fig. 2, *b*. It is seen that the optical transmission coefficients of the obtained films have the maxima in the wavelength range of 620–660 nm. Similar transmission spectra for the film structures, consisting of  $\text{Cu}_3\text{Se}_2$  or CuSe, were obtained in [33–35]. Figure 2, *b* shows that thermal annealing of the synthesized film causes an increase of its transmission coefficient in the wavelength region of  $560 < \lambda < 1100$  nm. It means that in the given spectral region the thin film, consisting of CuSe, is more transparent than the thin  $\text{Cu}_3\text{Se}_2$  film.

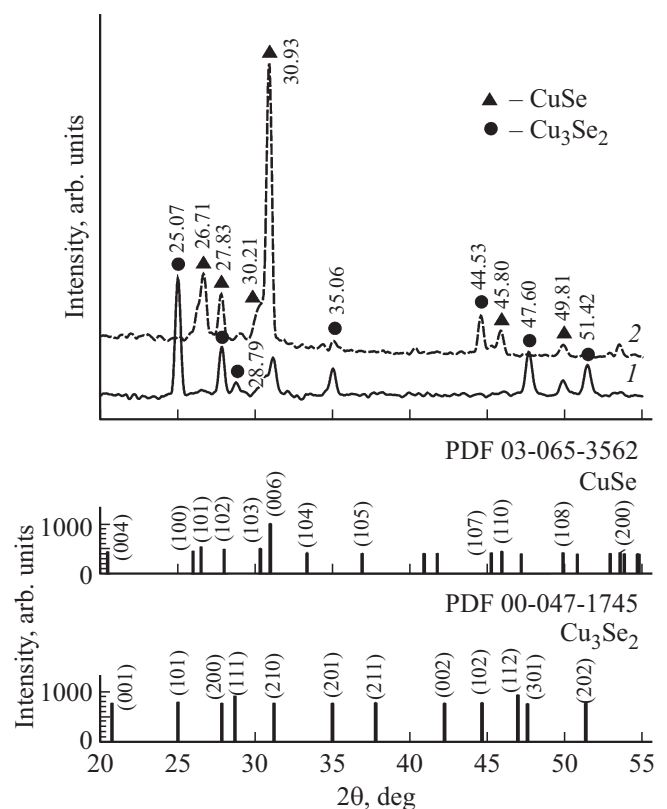


**Figure 3.** Diffraction patterns of the Se(45 nm)/Cu(90 nm) film structure after explosive crystallization (1) and their thermal annealing at  $140^{\circ}\text{C}$  for 30 min (2), as well as reference X-ray diffraction patterns and  $hkl$  of the found phases under excitation by X-ray radiation  $\text{CuK}\alpha$ .

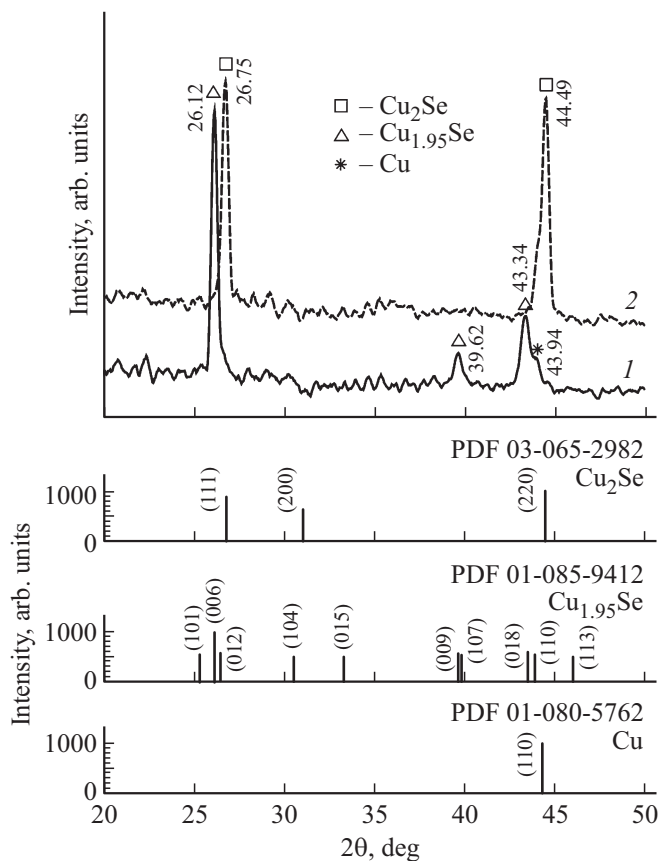


**Figure 4.** Diffraction patterns of the Se(45 nm)/Cu(115 nm) film structure after explosive crystallization (1) and their thermal annealing at 140°C for 30 min (2), as well as reference X-ray diffraction patterns and  $hkl$  of the found phases under excitation by radiation  $CuK_{\alpha}$ .

$E_g$  of the synthesized films was determined using the optical transmission spectra shown in Fig. 2, *b*. The obtained values of  $E_g$  for the composite  $Cu_3Se_2/CuSe/a$ -Se film (obtained before annealing) in regions of direct and indirect optical transitions were 2.03 and 1.68 eV respectively. After its heat treatment, a composite  $CuSe/Cu_3Se_2$  film forms (with the prevailing  $CuSe$  phase), whose values of  $E_g$  in regions of direct and indirect optical transitions were 2.11 and 1.93 eV, respectively.

Thus, a texturized polycrystalline nanocomposite film forms in the composite  $Cu_3Se_2/CuSe$  film after thermal annealing; this film consists of  $CuSe$  crystallites and a small amount of  $Cu_3Se_2$  crystallites. The film has a smaller absorbance in the wavelength region of  $560 < \lambda < 1100$  nm and a greater  $E_g$  in the regions of direct and indirect optical transitions.

Further increase of the Cu film thickness with an unchanged Se film thickness of 45 nm during the formation of a Se/Cu film structure causes a phase composition shift of the copper selenide film towards  $Cu_2Se$ . Thus, the diffraction pattern for the Se(45 nm)/Cu(115 nm) film structure obtained after explosive crystallization has diffraction

peaks that correspond to the lines of reflection from the rhombic  $Cu_{1.95}Se$  phase, pertaining to the space group of symmetry  $R\bar{3}m$  (PDF 01-085-9412) having the crystal lattice parameters  $a = 0.4123$  nm,  $c = 2.0449$  nm (Fig. 4, curve 1). This is confirmed by three scattering peaks with the angles  $2\theta = 26.12$ ,  $39.62$  and  $43.34^\circ$ . Subsequent thermal annealing of the synthesized  $Cu_{1.95}Se$  film at 140°C for 30 min causes an almost complete transition of the rhombic  $Cu_{1.95}Se$  phase into the cubic  $Cu_2Se$  phase having the crystal lattice parameter  $a = 0.5760$  nm. This is proved by the absence of the scattering peaks pertaining to  $Cu_{1.95}Se$  and formation of three intensive scattering peaks at the angles  $2\theta = 26.75$  and  $44.49^\circ$ , which correspond to the  $Cu_2Se$  phase (see Fig. 4, curve 2). According to the reference data, the  $Cu_2Se$  phase pertains to the space group of symmetry  $Fm\bar{3}m$  (PDF 03-065-2982). A comparison of the reference X-ray diffraction patterns and the recorded diffraction patterns in Fig. 4 shows that  $Cu_{1.95}Se$  crystallites during explosive crystallization grow predominantly in plane (006), while during thermal annealing  $Cu_2Se$  crystallites grow in planes (111) and (220). The transformation of  $Cu_{1.95}Se$  into  $Cu_2Se$  during thermal annealing can be explained by a solid-phase reaction during which the free Cu atoms, present in the film structure during vacuum-thermal deposition, interact chemically with  $Cu_{1.95}Se$  molecules to form  $Cu_2Se$ . Indeed, the diffraction pattern for the Se(45 nm)/Cu(115 nm) film structure after explosive crystallization (see Fig. 4, curve 1) has a Cu peak at the angle  $2\theta = 43.94^\circ$ . This peak is overlapped by a diffraction line with the angle  $2\theta = 43.34^\circ$ , which corresponds to  $Cu_{1.95}Se$  crystallites. The diffraction line of Cu in the angle  $2\theta = 43.94^\circ$  in the form of a pronounced branch can be also observed on the left side from the diffraction line of  $Cu_2Se$  with the angle  $2\theta = 44.49^\circ$  (see Fig. 4, curve 2). It means that free copper crystallites remain in the obtained film structure after annealing.

The optical transmission spectra for the synthesized Se(45 nm)/Cu(115 nm) film structure before and after thermal annealing are shown in Fig. 2, *c*. It is seen that the studied film structure becomes more transparent after annealing in the wide wavelength range from 400 to 1100 nm. This can be explained by a decreased concentration of Cu clusters in the annealed film, which significantly affect the film optical properties of the structure in the given wavelength range [36]. It can be noted that the film transmission coefficient at the wavelength of 800 nm after annealing increases from 30 to 52%. At the same time the annealed film in the short-wave region ( $\lambda < 600$  nm) features an abrupt decrease of the transmission coefficient with wavelength decrease, which agrees with the results in [37].

The data in Fig. 2, *c* was used to determine  $E_g$  for the synthesized films. The obtained values of  $E_g$  for the composite  $Cu_{1.95}Se/Cu$  film (obtained before annealing) in regions of direct and indirect optical transitions were 2.21 and 1.46 eV respectively. After its heat treatment, a composite  $Cu_2Se/Cu$  film forms, with the prevailing  $Cu_2Se$  phase, whose values

of  $E_g$  in regions of direct and indirect optical transitions were 2.33 and 1.92 eV respectively.

Thus, a polycrystalline  $\text{Cu}_{1.95}\text{Se}$  film, containing Cu particles, forms as a result of explosive crystallization in the Se(45 nm)/Cu(115 nm) film structure, obtained by the vacuum-thermal deposition method; this film almost fully transforms into a polycrystalline  $\text{Cu}_2\text{Se}$  film after thermal annealing.

#### 4. Conclusion

The method of vacuum-thermal evaporation during formation of a Se/Cu film structure was used to synthesize different composite films having different phase compositions. It has been shown that composite films simultaneously containing two  $\text{CuSe}/\text{Cu}_3\text{Se}_2$ ,  $\text{Cu}_{1.95}\text{Se}/\text{Cu}_2\text{Se}$ , as well as four Se/ $\text{Se}_8$ /CuSe/CuSe<sub>2</sub> crystalline phases can be obtained by changing the ratio of Se and Cu film thicknesses and by thermal annealing. It was found that thermal annealing of synthesized film structures at 140°C for 30 min leads to a considerable change in their optical transmission spectra. In case of direct optical transitions, values of  $E_g$  for the composite Se-Cu films, obtained after explosive crystallization and their subsequent thermal annealing, were 2.03–2.33 eV, and in case of indirect optical transitions they were 1.45–1.93 eV.

The suggested method for synthesis of composite copper selenide films does not require an ultra-high vacuum and high temperatures. Therefore, this method, thanks to its simplicity and technological effectiveness, can be used to obtain new materials in photonics and optoelectronics devices.

#### Funding

The work has been performed under the state assignment from the Ministry of Education and Science of Russia (No. of state reg. 1021032422167-7-1.3.2) and with financial support by the Russian Foundation for Basic Research (project No. 19-02-00112). This research has been conducted using the equipment at Shared Use Center „Center of Physical and Physicochemical Methods of Analysis and Study of Surface Properties and Characteristics, Nanostructures, Materials, and Products“ of the Udmurt Federal Research Center, Ural Branch of RAS.

#### Conflict of interest

The authors declare that they have no conflict of interest.

#### References

- [1] S.R. Gosavi, N.G. Deshpande, Y.G. Gudage, R. Sharma. *J. Alloys Compd.*, **448**, 344 (2008).
- [2] R. Yu, T. Ren, K. Sun, Z. Feng, G. Li, C. Li. *J. Phys. Chem. C*, **113**, 10833 (2009).
- [3] Y. Zhang, C. Hu, C. Zheng, Y. Xi, B. Wan. *J. Phys. Chem. C*, **114**, 14849 (2010).
- [4] Y. Zhang, Z.P. Qiao, X.M. Chen. *J. Mater. Chem.*, **12**, 2747 (2002).
- [5] V. Milman. *Acta Crystallogr. Sect. B*, **B58**, 437 (2002).
- [6] E.A. Fedorova, L.N. Maskayeva, V.F. Markov, V.I. Voronin, V.G. Bamburov. *Inorg. Mater.*, **55**, 106 (2019).
- [7] A.A. Ivanov, A.I. Sorokin, V.P. Panchenko, I.V. Tarasova, N.Yu. Tabachkova, V.T. Bublik, R.Kh. Akchurin. *Semiconductors*, **51**, 866 (2017).
- [8] Z. Zainal, S. Nagalingam, T.C. Loo. *Mater. Lett.*, **59**, 1391 (2005).
- [9] T. Liu, Y. Hu, W.B. Chang. *Mater. Sci. Eng. B*, **180**, 33 (2014).
- [10] F. Lin, G.Q. Bian, Z.X. Lei, Z.J. Lu, J. Dai. *Solid State Sci.*, **11**, 972 (2009).
- [11] Y.H. Lv, J.K. Chen, M. Döbeli, Y.L. Li, X. Shi, L.D. Chen. *J. Inorg. Mater.*, **30**, 1115 (2015).
- [12] V.S. Gurin, A.A. Alexeenko, S.A. Zolotovskaya, K.V. Yumashv. *Mater. Sci. Eng. C*, **26**, 952 (2006).
- [13] L.N. Maskayeva, E.A. Fedorova, V.F. Markov, M.V. Kuznetsov, O.A. Lipina, A.V. Pozdin. *Semiconductors*, **52**, 1334 (2018).
- [14] V.Ya. Kogay, A.V. Vakhrushev, A.Yu. Fedotov. *JETP Lett.*, **95**, 454 (2012).
- [15] V.Ya. Kogay, G.M. Mikheev. *Tech. Phys. Lett.*, **46**, 439 (2020).
- [16] G.M. Mikheev, V.Ya. Kogay, R.G. Zonov, K.G. Mikheev, T.N. Mogileva, Y.P. Svirko. *JETP Lett.*, **109**, 11, 704 (2019).
- [17] G.M. Mikheev, V.Y. Kogay, T.N. Mogileva, K.G. Mikheev, A.S. Saushin, Y.P. Svirko. *Appl. Phys. Lett.*, **115**, 061101 (2019).
- [18] G.M. Mikheev, V.Y. Kogay, K.G. Mikheev, T.N. Mogileva, A.S. Saushin, Y.P. Svirko. *Mater. Today Commun.*, **21**, 100656 (2019).
- [19] G.M. Mikheev, V.Y. Kogay, K.G. Mikheev, T.N. Mogileva, A.S. Saushin, Y.P. Svirko. *Opt. Express*, **29**, 2112 (2021).
- [20] G.M. Mikheev, A.E. Fateev, V.Y. Kogay, T.N. Mogileva, V.V. Vanyukov, Y.P. Svirko. *Appl. Phys. Lett.*, **118**, 201105 (2021).
- [21] P.P. Hankare, A.S. Khomane, P.A. Chate, K.C. Rathod, K.M. Garadkar. *J. Alloys Compd.*, **469**, 478 (2009).
- [22] V.M. Garcia, P.K. Nair, M.T.S. Nair. *J. Cryst. Growth*, **203**, 113 (1999).
- [23] O. Arellano-Tánori, M.C. Acosta-Enríquez, R. Ochoa-Landín, R. Iñiguez-Palomares, T. Mendívil-Reynoso, M. Flores-Acosta, S.J. Castillo. *Chalcogenide Lett.*, **11**, 13 (2014).
- [24] A. Jagminas, R. Juškeenas, I. Gailiute, G. Statkute, R. Tomašiunas. *J. Cryst. Growth*, **294**, 343 (2006).
- [25] D. Patidar, N.S. Saxena. *J. Cryst. Growth*, **343**, 68 (2012).
- [26] A.B. Lebed', S.S. Naboychenko, V.A. Shunin. *Proizvodstvo selena i tellura na OAO „Uraljelektrome“* (Yekaterinburg, Izd-vo Ural. un-ta, 2015) (in Russian).
- [27] A.V. Lyubchenko. *Fizicheskiye osnovy poluprovodnikovoy infrakrasnoy fotoelektroniki* (Kiev, Nauk. dumka, 1984) (in Russian).
- [28] A. El-Denglawey, M.M. Makhlof, M. Dongol. *Results Phys.*, **10**, 714 (2018).
- [29] V.Ya. Kogay. *Tech. Phys. Lett.*, **44**, 1002 (2018).
- [30] E.V. Aleksandrovich, E.V. Stepanova, A.V. Vakhrushev, A.N. Aleksandrovich, D.L. Bulatov. *ZhTF*, **83**, 50 (2013) (in Russian).

- [31] V.Ya. Kogay. *Tech. Phys. Lett.*, **40**, 636 (2014).
- [32] E.V. Aleksandrovich, A.N. Aleksandrovich, G.M. Mikheev. *J. Non-Cryst. Sol.*, **545**, 120249 (2020).
- [33] M. Lakshmi, K. Bindu, S. Bini, K.P. Vijayakumar, C.S. Kartha, T. Abe, Y. Kashiwaba. *Thin Sol. Films*, **386**, 127 (2001).
- [34] B. Pejova, I. Grozdanov. *J. Solid State Chem.*, **158**, 49 (2001).
- [35] I.G. Shitu, J.Y.C. Liew, Z.A. Talib, H. Baqiah, M.M.A.K. Kechik, M.A.K. Kamarudin, N.H. Osman, Y.J. Low, I.I. Lakin. *ACS Omega*, **6**, 10698 (2021).
- [36] B. Maack, N. Nilius. *Corros. Sci.*, **159**, 108112 (2019).
- [37] H. Ahn, Y. Um. *J. Korean Phys. Soc.*, **64**, 1600 (2014).